2024 IEEE International Conference on Robotics and Automation (ICRA 2024)
May 13-17, 2024. Yokohama, Japan

Self-Righting Shell for Robotic Hexapod

Katelyn King[1] and Shai Revzen[2]

[1]Department of Biomedical Engineering, Robotics Institute, University of Michigan, Ann Arbor
[2]Department of Electrical Engineering and Computer Science, Department of Ecology and Evolutionary Biology, University of Michigan, Ann Arbor

***Abstract*—Decimeter scale robots in human environments are small relative to obstacles they encounter, making them prone to flipping over and needing to self-right. We present a multi-faceted shell that by its geometry alone enables the hexapedal robot MediumANT to passively self-right without the need for additional sensory feedback. We designed the shell by specifying the cross-sectional geometry in the yz and xy planes such that the robot returns to an upright position by rolling around the longitudinal (x) axis, and then tweaked the design to reduce the number of faces. We then attached the shell to the robot by modifying some of its chassis structural plates to extend to and support the shell. We evaluated the effectiveness of the shell in two experimental scenarios: passive righting – balancing the robot on each face of the shell before releasing the robot – and an intentional fall – walking the robot off a ledge at various approach angles. As intended by our design, the robot recovered the upright orientation from all starting faces in the passive righting test and righted itself and continued walking in all falling trials. This work presents an example of using biologically inspired simplicity to solve what would otherwise be a technically challenging problem.**

***Index Terms*—self-righting, multi-legged, robot**

I. Introduction

Decimeter scale robots moving through human environments face a terrain which is extremely rough relative to their scale. There are many obstacles, such as stairs, boxes, and furniture, which are taller than the robot is long. Even if the robot climbs down from the obstacle, it is likely to land on a face other than that containing locomotor appendages such as legs and wheels. Despite this, small robots rarely self-right on their own [1]. This is owing to such robots having wheels or legs that are small relative to their body size, rendering active self-righting ineffective. Common among larger legged robots, active mechanisms of self-righting require a controller to coordinate the movement of modules or appendages. Modular approaches include the self-righting backbone of the SRR-II [2] and cooperation among VelociRoACH robots [3] whereby team members push over inverted comrades [4]. Self-righting robots with appendages imitate biological adaptations such as legs, tails, and wings. RoboCrab, a robot designed for surf zone exploration, automatically rights itself with a tail mimicking that of a horseshoe crab [5]. The legged VelociRoACH robot employs a similar tail for navigating terrestrial environments [6]. Another legged robot, RHex, uses actuated limbs to reorient itself via a front or back flip [7]. A winged strategy observed in cockroaches has also been implemented using the VelociRoACH [8].

Common to the majority of these methods is a rounded shell from which an inverted robot may push off into its upright position. The body covering of RoboCrab mimics the rounded geometry of a horseshoe crab shell, enabling the robot to roll and ultimately self-right using a combination of tail and leg movements [5]. The wheeled-legged robot NOROS consists of six appendages which extend radially from a hemispherical shell, allowing the inverted robot to roll along its shell while its legs execute a self-recovery routine [9]. Among VelociRoACH teams, each member's rounded shell is essential to enabling teammates to push over inverted companions [4].

Rather than utilizing shells cooperatively with sensors and controllers, self-righting systems may be greatly simplified by relying on shell geometry alone. Li et al. highlight the need to consider body shape as a means of improving robot mobility without the need for additional sensory feedback [10]. By adding a rounded shell, the group enabled a legged robot to traverse beam obstacles without modifying the robot's controller or sensing architecture. Such designs already exist in nature, among which turtle and beetle shell geometries have been studied in depth. Turtles with highly domed shells can self-right without any effort; thus, these shells are common among turtles with short limbs and necks and hence no means of active control [11]. Of note is the resemblance between the shell of the Indian Star Tortoise and the Gömböc, a three-dimensional, homogeneous, convex, mono-monostatic body with just one stable and one unstable equilibrium [12]. When resting on a flat surface, both shapes settle on their only stable configuration, which for an Indian Star Tortoise is on its feet. Being neither mono-monostatic nor homogeneous, the tortoise shell is simplified compared to the Gömböc, yet still achieves the desired self-righting behavior.

II. Problem Statement

Here we present a multi-faceted shell that by its geometry alone enables the hexapedal robot MediumANT to passively self-right on level ground without the need for additional sensory feedback. As a secondary goal, this shell was designed to comprise flat faces, and reduce the number of such faces, so as to ease the process of manufacturing the shell out of laser cut parts. We designed this shell to operate on level

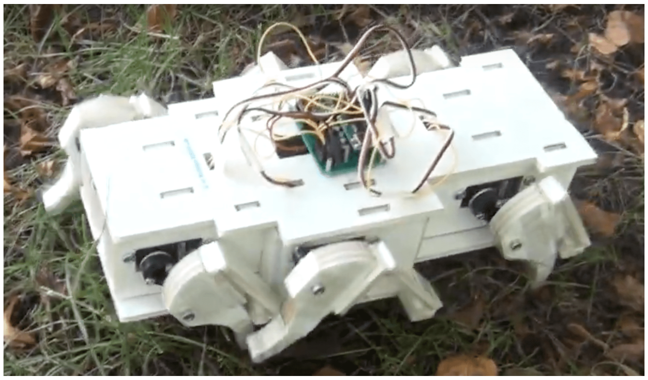

Fig. 1: Original MediumANT robot without shell

ground, as small robots have begun expanding into the structured environments in which humans work and live, including homes, hospitals, and industrial settings where most surfaces the robot might land on are level [13].

III. Robot Design

A. MediumANT Robot

The MediumANT robot is an open-source design released as part of NSF CMMI grant #182591 (Figure 1). We fabricated the robot according to the instructions at https://mileggedrobots.eecs.umich.edu/index.php/mediumant/, with slight modifications. We installed a pair of median plates along the center line of the robot beneath the top plate (Figure 2a). We also mounted the battery pack on the base plate by adding a pair of small ribs positioned between and perpendicularly to the existing front and median ribs. We placed the battery pack battery-side down between the new ribs, flush with the median rib. These changes lowered the center of mass, prevented the battery from shifting when the robot rocked to either side, and enabled the batteries to be replaced through an opening on the underside of the robot.

The following discussion references the axes shown in Figure 2a, as well as the robot's coronal, axial, and sagittal planes. Consistent with their anatomical definitions, we used these terms to refer to the planes orthogonal to the roll (x), yaw (z), and pitch (y) axes, respectively. We define multiple sagittal (xz) planes such that the median plane bisects the robot and parasagittal planes are off-center.

B. 2D Shell Geometry

We designed the shell to allow the robot to return to an upright position by rolling around the longitudinal (x) axis (Figure 2a). We achieved this by designing the coronal plates such that the perpendicular bisector of each plate edge was tangent to a circle of fixed radius centered at the robot's center of mass (Figure 3a). Relying on the approximation that the effective line of force exerted by a flat face on level ground is approximately normal to the face and through the centroid of the face, our choice guaranteed that any such force would have a lever arm around the center of mass (CoM) and exert a moment righting the robot. Using a pre-existing model of MediumANT in Autodesk Inventor 2022, we drew the bottom edge of the coronal plate co-linear with the lower edge of the robot's bottom plate so the shell would not inhibit the robot's range of motion in the vertical plane (Figure 2b). We chose to make the plate left-right symmetric.

We realized our design with three coronal plate edge segments on each side; fewer resulted in a much larger shell. We constrained (using AutoDesk Inventor sketch constraints) the first segment to start co-incident with the end of the base edge, which we chose slightly wider than the existing width of the robot. We constrained last edge to end on the plate's axis of symmetry. To produce the desired self-righting moments we also constrained the perpendicular bisector of each edge tangent to a circle we drew around the CoM. After we manually adjusted the edge endpoints, all three edges were of approximately equal length.

This geometry theoretically enables the robot to self-right on up to 16° of incline, regardless of which faces it lands on (Figure 3c). This angle is a function of the (1) distance (d) from the midpoint of the top face to the point of tangency between the perpendicular bisector of the top face and the circle we drew around the CoM and (2) the radius (r) of this circle.

C. 3D Shell Model

The 3D shell design consists of three sections, where the self-righting coronal plates compose the midsection, and the front and rear sections are designed to divert the robot onto the sides of the midsection so it may self-right. The design of the front and rear sections were refined iteratively during testing until the shell survived falling from a height of about one meter. A viable 3D shell thus needed to be manufacturable and strong enough to withstand the expected impacts, but not contain so much mass as to disrupt the self-righting functionality by moving the CoM too high.

We designed the 3D shell by specifying the cross-sectional geometry in the yz and xy planes, using the coronal plate as the yz cross-section (Figure 3a). We designed the horizontal plane (xy) cross-section with angled faces at the front and rear to divert the robot around obstacles (Figure 3b). By making this shape symmetric about its horizontal (x) and vertical (z) center lines we positioned its centroid at the intersection of these axes.

Our initial attempt at a shell was an actual shell based on the solid produced from intersecting prisms with the desired xy and yz cross-sections (Figure 5a). However, this shell proved to have so much material that the CoM moved far enough to preclude self-righting from some faces.

Instead, we built a design based on internal plates, with a full shell only in the lower part of the front and back. The advantage of this implementation was reducing the material at the shell's periphery while loading the plates along their strongest axes.

After placing the coronal plates and bracing them in the x direction, we installed parasagittal plates to stabilize

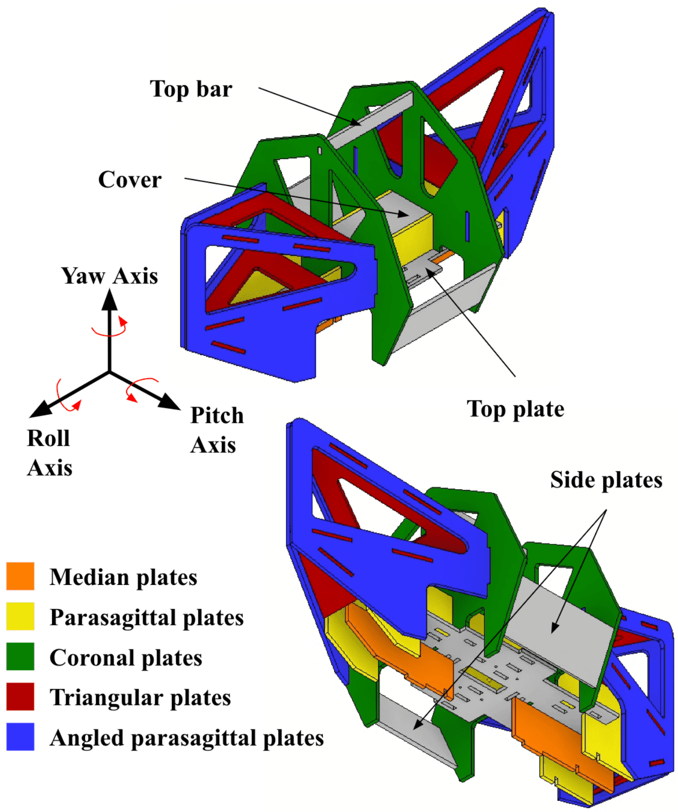

(a) Shell structure and axes

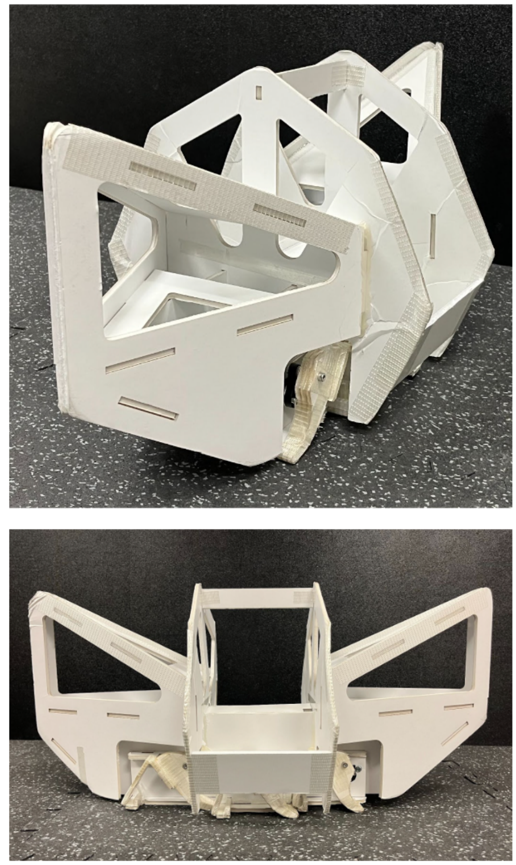

(b) MedANT with shell

Fig. 2: Robot axes

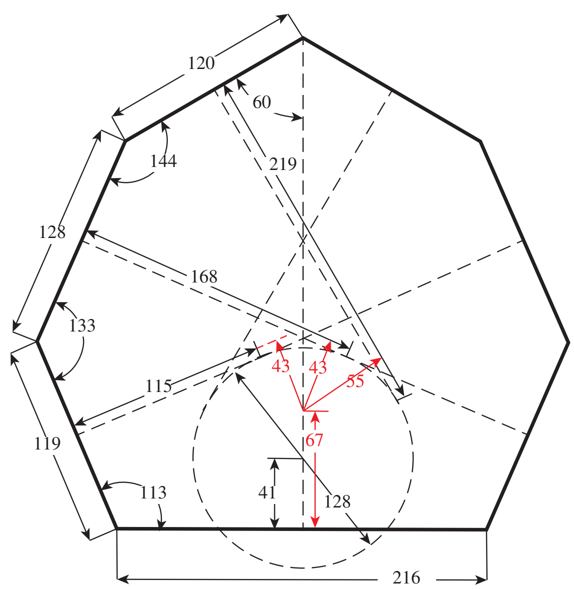

(a) Coronal plate geometry with measured CoM and estimated lever arms in red.

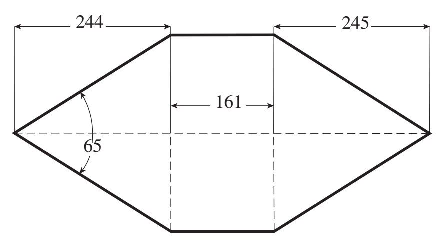

(b) Top-down geometry.

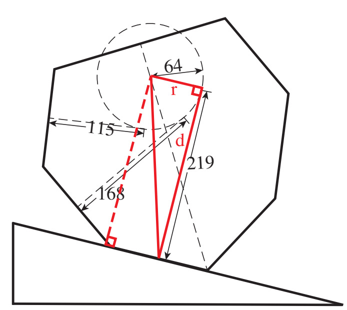

(c) Maximum incline ($atan(r/d) \approx 16°$).

Fig. 3: 2D shell geometry. Lengths in mm. Angles in degrees.

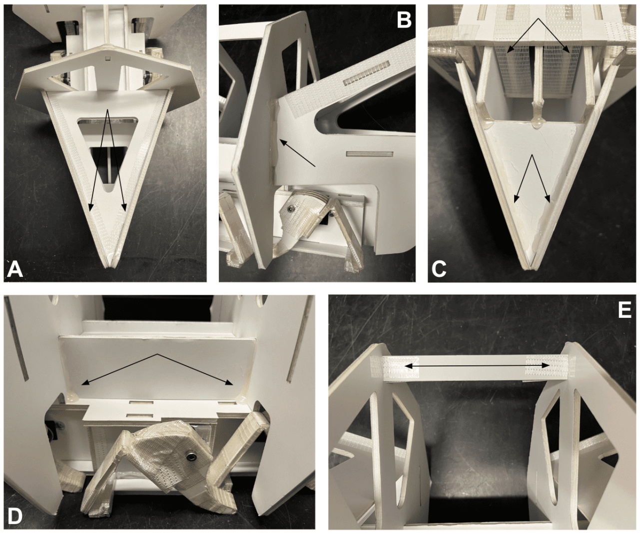

Fig. 4: Shell assembly showing areas of reinforcement

the rest of the structure. We designed angled parasagittal plates to maintain the desired xy projection with tapering front and back (Figure 3b). We reinforced these plates with three triangular plates fitted between each pair of angled parasagittal plates.

To further reduce the weight of the shell, we drew lines from the CoM to each corner of the (convex) shell, and projected these lines on the plates containing those corners. We preserved the material surrounding these projected lines to maintain the shell's compression resistance, but removed material elsewhere, with a focus on removing shell material that is "above" the CoM.

D. Assembly

We cut the structural plates for the shell from White Elmer's foam core (3/16") using a PLS6.150D model laser cutter from Universal Laser Systems. With the MediumANT fully constructed via the method linked above, we built the shell atop the robot in three sections: mid, front, and rear. We constructed the midsection of the robot by slotting the parasagittal plates into the top plate, followed by the coronal plates into the parasagittal plates. We then fit the top bar and side plates between the coronal plates and secured them with fiber tape (Scotch #8959) (Figure 4E). To construct the front and rear of the robot, we slotted three triangular plates between the corresponding angled parasagittal plates. We joined all three section by slotting the tabs at the back of the angled parasagittal plates into the corresponding slots in the coronal plates. We secured the joints with hot glue (Figure 4B). To reinforce the shell, we placed fiber tape along the junction between the top triangular plates and angled parasagittal plates at the front and rear of the shell (Figure 4A). We secured the shell to the robot by wrapping fiber tape from the bottom to the top plate around the front and rear of the robot, as well as from the bottom plate to the angled parasagittal plates underneath the front and rear of the

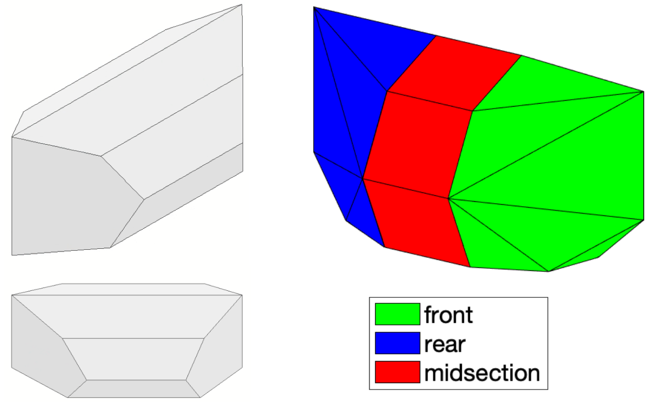

(a) Solid shell design. (b) Convex hull.

Fig. 5: 3D shell geometry.

shell (Figure 4C, top set of arrows). To strengthen the shell, we applied hot glue to the corners formed by the coronal plate and parallel parasagittal plates Figure 4D), as well as to the junction between the bottom triangular plate and angled parasagittal plates at the front and rear of the shell Figure 4C, bottom set of arrows).

IV. Self-Righting Experiments

We evaluated the effectiveness of the shell in two experimental scenarios. The first scenario involved passive righting – balancing the robot on each face of the shell, releasing the robot, and observing whether self-righting was successful. The second scenario was an intentional fall – we walked the robot off a ledge at various approach angles and examined its ability to self-right after falling from a ledge.

A. Passive Righting

We identified shell faces by fitting a convex hull to the set of corners on the periphery of the shell. We programmed a brute force algorithm [14] in Matlab to visualize a convex hull, which yielded fifteen unique faces, including six coronal, six rear, and three side faces each composed of a set of three vertices (Figure 5b). Due to the symmetry of the shell about its median plane, twenty-eight faces existed in all. Testing consisted of twenty-eight trials, each of which tested one face of the robot. In each trial, we held the robot stationary using a rod, with its legs retracted, and one face contacting the ground. We then quickly removed the rod balancing the robot and observed whether the robot succeeded in self-righting. By holding the robot with a rod we reduced the likelihood that we unintentionally impart the robot with momentum when releasing it.

B. Intentional Fall

We walked the robot off a ledge that was 1 meter above the ground starting from one of five orientations (Figure 6). The height of the drop was sufficiently high to allow the

(a) Test setup (front) with world frame

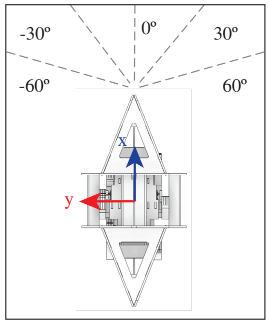

(b) Test setup (top) with body frame

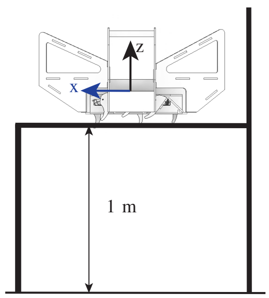

(c) Test setup (side) with body frame

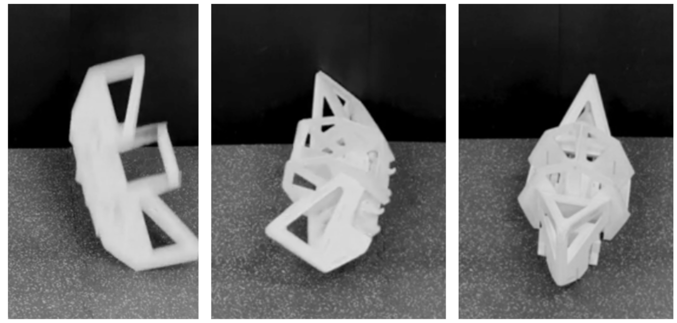

(d) Trial A: Impact, Self-Righting, Upright

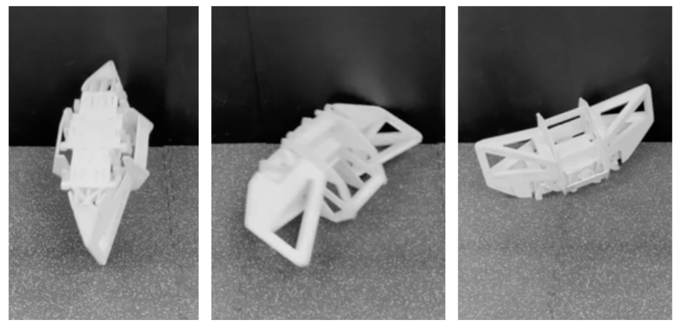

(e) Trial B: Impact, Self-Righting, Upright

Fig. 6: Falling test

robot to tumble, thereby allowing it to land on any face. We conducted a total of 15 trials, including 3 trials in each of 5 orientations ranging from -60°to +60°in 30°increments (Figure 6b). In the 0°orientation, we measured the robot's motion as it tumbled using the Qualisys Motion Capture Camera System with 10 cameras and 9 reflective markers arranged randomly on the sides of the MediumANT shell. We used the measured three-dimensional marker positions to compute the robot's linear velocity in the world frame and angular velocity in the body frame. The orientations of the world and body frame are shown in Figure 6.

V. Discussion

As intended by our design, the robot righted itself and continued walking in all 15 trials and recovered the upright orientation from all starting faces in the passive righting test. We designed the shell to force the robot to land on its side after tumbling, thereby allowing the robot to self-right due to the moments created by the geometry of the mid-section of the shell. This mechanism of action is demonstrated in the results of our motion capture analysis of the robot during the intentional fall trials. The angular velocity plot in Figure 7 is dominated by rotation about the roll axis (Rx), showing the robot rolling onto its right side and back to the left before coming to rest on its base. Rotation about the other axes (Ry, Rz) is observed towards the beginning of the trial while the robot is tumbling, but diminishes throughout the self-righting phase of the motion. Also, linear velocity along the world x-axis changes linearly during self-righting, illustrating the constant torque the robot experiences during self-righting due to the shell geometry. These results demonstrate that a little bit of mechanical design can go a long way towards making small robots robust and reliable to failures such as falling or landing upside-down.

While many robot designers move to address failure modes by adding actuated DoF or sophisticated controllers, this may well be an expression of the cognitive bias towards solving problems by adding rather that removing or changing components [15]. In the natural world, many environmental interactions related to locomotion are resolved bio-mechanically without the need for modulating the neural controls. This has been shown in a variety of ways for cockroaches [16], [17], [18] and can be shown mathematically to be possible in a large range of systems [19].

Our work here presents an example of using biologically inspired simplicity to solve what would otherwise be a technically challenging problem. Even with our shell, the robot cannot self-right under all conditions. Specifically, when landing on a non-flat surface of sufficient curvature in an unfortunate orientation, the robot with the shell we designed might roll into an obstacle and get stuck.

There is no universal way to prevent a robot from getting stuck after tumbling into an arbitrary object (consider, e.g. tumbling into a raspberry bush with inward pointing thorns). What we have shown is that the most common type of righting needed in man-made environments can be addressed

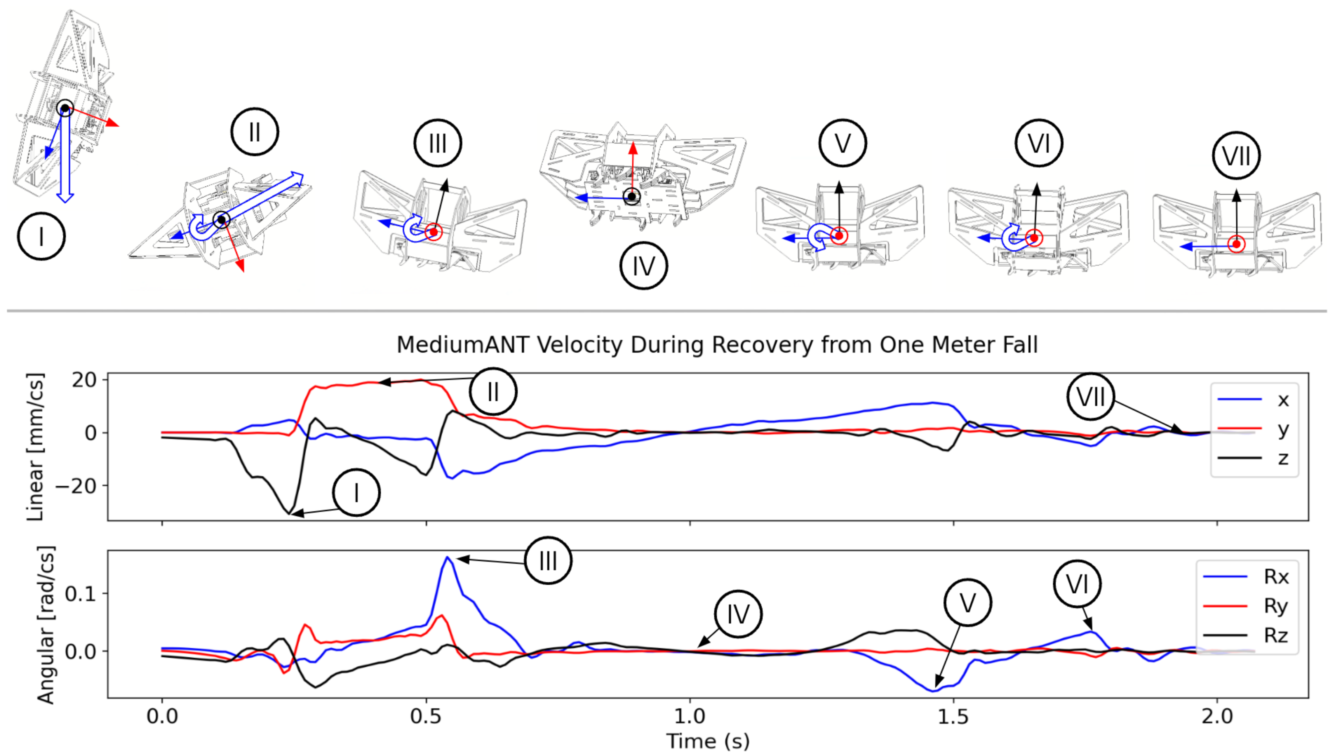

Fig. 7: Time series of robot linear velocity in world frame and angular velocity in body frame after falling one meter. In this example, first the robot falls with negative velocity along the world z-axis (I). Once it hits the ground, the robot bounces and flies through the air with a constant velocity along the world y-axis (II). The robot simultaneously begins to roll about the body x-axis and continues to roll as it again hits the ground (III). The robot then stops on its right side (IV) before rolling back over to the left (V). It rolls past the base onto its left side, so a small rock back to the right is observed (VI) before the robot comes to rest on its base (VII).

using a purely passive mechanical design. Even if the robot has additional actuators that may help in righting in more extreme cases, when using a shell such as ours is possible it allows the robot to reserve the use of those actuators for those extreme cases.

A natural evolution of this project is to improve the strength-to-weight ratio of the shell, to tweak the design to work on a greater variety of surfaces, and to otherwise reshape the shell to obtain additional desirable properties such as those described in [10].

Acknowledgment

We would like to thank Hao Lou for his work on designing the original MediumANT. This work has been funded in part by ARO MURI W911NF-17-1-0306, NSF CMMI 1825918, NSF CPS 2038432, and the D. Dan and Betty Kahn Michigan-Israel Partnership for Research and Education Autonomous Systems Mega-Project.

References

[1] C. Li, C. C. Kessens, R. S. Fearing, and R. J. Full, “Mechanical principles of dynamic terrestrial self-righting using wings,” *Advanced Robotics*, vol. 31, no. 17, pp. 881–900, 2017.

[2] J. Qian, W. Cheng, Y. He, J. Su, and Y. Zhang, “A novel mobile robot with a backbone for self up-righting capability,” in *Proceedings. 2000 IEEE/RSJ International Conference on Intelligent Robots and Systems (IROS 2000)(Cat. No. 00CH37113)*, vol. 3. IEEE, 2000, pp. 2224–2229.

[3] D. W. Haldane, K. C. Peterson, F. L. G. Bermudez, and R. S. Fearing, “Animal-inspired design and aerodynamic stabilization of a hexapedal millirobot,” in *2013 IEEE international conference on robotics and automation*. IEEE, 2013, pp. 3279–3286.

[4] D. L. McPherson and R. S. Fearing, “Team-based robot righting via pushing and shell design,” in *2019 International Conference on Robotics and Automation (ICRA)*. IEEE, 2019, pp. 2168–2173.

[5] G. Krummel, K. N. Kaipa, and S. K. Gupta, “A horseshoe crab inspired surf zone robot with righting capabilities,” in *International Design Engineering Technical Conferences and Computers and Information in Engineering Conference*, vol. 46360. American Society of Mechanical Engineers, 2014, p. V05AT08A010.

[6] C. S. Casarez and R. S. Fearing, “Dynamic terrestrial self-righting with a minimal tail,” in *2017 IEEE/RSJ International Conference on Intelligent Robots and Systems (IROS)*. IEEE, 2017, pp. 314–321.

[7] U. Saranli, A. A. Rizzi, and D. E. Koditschek, “Model-based dynamic self-righting maneuvers for a hexapedal robot,” *The International Journal of Robotics Research*, vol. 23, no. 9, pp. 903–918, 2004.

[8] C. Li, C. C. Kessens, A. Young, R. S. Fearing, and R. J. Full, “Cockroach-inspired winged robot reveals principles of ground-based dynamic self-righting,” in *2016 IEEE/RSJ International Conference on Intelligent Robots and Systems (IROS)*. IEEE, 2016, pp. 2128–2134.

[9] S. Peng, X. Ding, F. Yang, and K. Xu, “Motion planning and implementation for the self-recovery of an overturned multi-legged robot,” *Robotica*, vol. 35, no. 5, pp. 1107–1120, 2017.

[10] C. Li, A. O. Pullin, D. W. Haldane, H. K. Lam, R. S. Fearing, and R. J. Full, “Terradynamically streamlined shapes in animals

and robots enhance traversability through densely cluttered terrain," *Bioinspiration & biomimetics*, vol. 10, no. 4, p. 046003, 2015.
[11] G. Domokos and P. L. Várkonyi, "Geometry and self-righting of turtles," *Proceedings of the Royal Society B: Biological Sciences*, vol. 275, no. 1630, pp. 11–17, 2008.
[12] P. L. Várkonyi and G. Domokos, "Mono-monostatic bodies: the answer to arnold's question," *Math. Intelligencer*, vol. 28, no. 4, pp. 34–38, 2006.
[13] M. Ben-Ari, F. Mondada, M. Ben-Ari, and F. Mondada, "Robots and their applications," *Elements of robotics*, pp. 1–20, 2018.
[14] F. Yaacoub, Y. Hamam, A. Abche, and C. Fares, "Convex hull in medical simulations: A new hybrid approach," in *IECON 2006 - 32nd Annual Conference on IEEE Industrial Electronics*, 2006, pp. 3308–3313.
[15] G. S. Adams, B. A. Converse, A. H. Hales, and L. E. Klotz, "People systematically overlook subtractive changes," *Nature*, vol. 592, no. 7853, pp. 258–261, 2021.
[16] D. L. Jindrich and R. J. Full, "Dynamic stabilization of rapid hexapedal locomotion," *J Exp Biol*, vol. 205, no. 18, pp. 2803–2823, Sep 2002.
[17] D. M. Dudek and R. J. Full, "An isolated insect leg's passive recovery from dorso-ventral perturbations," *J Exp Biol*, vol. 210, no. 18, pp. 3209–3217, SEP 15 2007.
[18] S. Revzen, S. A. Burden, T. Y. Moore, J.-M. Mongeau, and R. J. Full, "Instantaneous kinematic phase reflects neuromechanical response to lateral perturbations of running cockroaches," *Biol Cybern*, vol. 107, no. 2, pp. 179–200, 2013.
[19] G. Council, S. Yang, and S. Revzen, "Deadbeat control with (almost) no sensing in a hybrid model of legged locomotion," in *Advanced Mechatronic Systems (ICAMechS), 2014 International Conference on*. IEEE, Aug 2014, pp. 475–480.